

This article is published as part of the *Dalton Transactions* themed issue entitled:

## New Talent

*Showcasing the strength of research being carried out by tomorrow's leaders in the field of inorganic chemistry*

Guest Editor Polly Arnold  
University of Edinburgh, UK

Published in [issue 2, 2010](#) of *Dalton Transactions*



Image reproduced with permission of Mark Muldoon

Articles in the issue include:

### PERSPECTIVES:

[Modern multiphase catalysis: new developments in the separation of homogeneous catalysts](#)

Mark J. Muldoon, *Dalton Trans.*, 2010, DOI: 10.1039/b916861n

[Probing bioinorganic chemistry processes in the bloodstream to gain new insights into the origin of human diseases](#)

Elham Zeini Jahromi and Jürgen Gailer, *Dalton Trans.*, 2010, DOI: 10.1039/b912941n

### COMMUNICATIONS:

[Facile entry to 3d late transition metal boryl complexes](#)

Ba L. Tran, Debashis Adhikari, Hongjun Fan, Maren Pink and Daniel J. Mindiola, *Dalton Trans.*, 2010, DOI: 10.1039/b912040h

[Probing the kinetics of ligand exchange on colloidal gold nanoparticles by surface-enhanced raman scattering](#)

Yuhua Feng, Shuangxi Xing, Jun Xu, Hong Wang, Jun Wei Lim and Hongyu Chen, *Dalton Trans.*, 2010, DOI: 10.1039/b912317b

Visit the *Dalton Transactions* website for more cutting-edge inorganic and organometallic research  
[www.rsc.org/dalton](http://www.rsc.org/dalton)

# Mono-alkylated bisphosphines as dopants for ESI-MS analysis of catalytic reactions†

Danielle M. Chisholm,<sup>a</sup> Allen G. Oliver<sup>b</sup> and J. Scott McIndoe<sup>\*a</sup>

Received 3rd July 2009, Accepted 21st September 2009

First published as an Advance Article on the web 14th October 2009

DOI: 10.1039/b913225b

Bisphosphines  $\text{Ph}_2\text{P}(\text{CH}_2)_n\text{PPh}_2$  ( $n = 1, 2, 4, 6$ ) may be easily monobenzylated to generate cationic phosphine/phosphonium ligands  $[\text{Ph}_2\text{P}(\text{CH}_2)_n\text{PPh}_2\text{CH}_2\text{Ph}]^+$ . These ligands may be doped into a catalytic reaction involving neutral complexes with labile phosphine ligands, and replacement of a neutral phosphine with a charged analogue renders the resulting complex amenable to electrospray ionisation mass spectrometry (ESI-MS). Examination of olefin hydrogenation with Wilkinson's catalyst,  $\text{RhCl}(\text{PPh}_3)_3$ , revealed that this approach yielded rapid identification of all off-cycle solution species as well as catalyst poisons. Reactive intermediates could be generated using collision-induced dissociation (CID) of a triphenylphosphine ligand to make three-coordinate  $\text{RhClP}_2$  species, and these react with alkenes in the gas phase to form  $\text{RhClP}_2(\text{alkene})$ . The solution speciation and gas phase behaviour revealed by ESI-MS match closely to what is already known about the system from kinetic and NMR studies.

## Introduction

We develop tools to facilitate electrospray ionization mass spectrometry (ESI-MS) analysis of organometallic compounds, and use them to probe catalytic reactions.<sup>1-4</sup> ESI-MS involves injecting a solution through a charged capillary, and upon emerging, the solution breaks apart into a spray of fine droplets.<sup>5</sup> A warm bath gas evaporates the solvent, and the ions evaporate from the droplets and are drawn into the mass spectrometer through a series of differentially pumped chambers. ESI is a soft ionization technique insofar as ion fragmentation tends to be minimal, but essentially serves to transport preformed ions from solution into the gas phase.<sup>6</sup> Its application in the study of catalytic systems is becoming increasingly popular,<sup>7-13</sup> and its utility has been extended from a characterization method to a reaction chamber through studying gas-phase ion-molecule chemistry.<sup>14-16</sup> The best results in ESI-MS come from ionic compounds, though neutral molecules can also be detected through weak interactions with charged species (typically protonation or cationization to form *e.g.* an  $[\text{M} + \text{H}]^+$  pseudomolecular ion); effectively, species of interest need to be preionized in solution or have a reasonably high gas-phase basicity.<sup>17</sup> To facilitate the study of catalytic reactions, where intermediates of interest may be present in very low concentration, very high ionization efficiency is crucial to the success of the experiment.

The functionalization of phosphines is a popular topic in inorganic and organometallic chemistry, and is carried out most frequently with the intent of altering the steric and electronic

properties of the ligand, often including conferring chirality on the metal complex and enabling it to perform asymmetric catalysis. Phosphines are often components of hemilabile chelating ligands with mixed donor sets.<sup>18,19</sup> Efforts have also been made to alter the solubility properties of phosphine ligands, for example by appending fluororous "ponytails" to make the ligands (and their complexes) soluble in fluororous solvents.<sup>20</sup> Because phosphines are amenable to functionalization, they are a good ligand with which to attach a charge. Various strategies have been employed to this end, most involving a series of functionalization/protection/quaternisation/deprotection steps.<sup>21</sup>

Ligands that render complexes amenable to ESI-MS have been introduced by Henderson and co-workers, who described the syntheses and characterization of the phosphines  $\text{PPh}_n(p\text{-C}_6\text{H}_4\text{OMe})_{(3-n)}$  and  $\text{PPh}_n(p\text{-C}_6\text{H}_4\text{NMe}_2)_{(3-n)}$  ( $n = 0-3$ ) and the arsine  $\text{As}(p\text{-C}_6\text{H}_4\text{OMe})_3$ , which may be coordinated to metal carbonyl complexes and are readily detectable by ESI-MS as the  $[\text{M} + \text{H}]^+$  ions.<sup>22</sup> To enhance the ionization efficiency in order to facilitate the analysis of catalytic reactions, we have prepared proton sponge-derivatized phosphines, where the 1,8-dimethylaminonaphthalene structure provides a highly basic and selective site for proton uptake to form  $[\text{M} + \text{H}]^+$  ions, with ionization efficiency close to that of permanently charged ions.<sup>23</sup> In a similar vein, we have described a simple synthesis of bisphosphine monoxides,  $\text{Ph}_2\text{P}(\text{O})(o\text{-C}_6\text{H}_4)\text{PR}_2$  ( $\text{R} = \text{aryl or alkyl}$ ), in which the pendant phosphine oxide has a high affinity for alkali metal ions, providing *e.g.*  $[\text{M} + \text{Na}]^+$  ions for easy analysis.<sup>24</sup>

A one-step synthesis of a permanently charged phosphine ligand has remained a desirable goal for us, and accordingly we explored a preparation that was first published in 1969: the monoalkylation of bisphosphines to form phosphine/phosphonium ligands.<sup>25</sup> A wide variety of bisphosphines are commercially available, most commonly  $\text{Ph}_2\text{P}(\text{CH}_2)_n\text{PPh}_2$  ( $n = 1-6$ ; commonly abbreviated *dppm*, *dppe*, *dppp*, *etc.*) but including numerous others and also a handful of trisphosphines. There are, of course, also many other more elaborate chiral bisphosphines available designed

<sup>a</sup>Department of Chemistry, University of Victoria, P.O. Box 3065, Victoria, BC V8W 3V6, Canada. E-mail: mcindoe@uvic.ca

<sup>b</sup>Department of Chemistry and Biochemistry, University of Notre Dame, 251 Nieuwland Science Hall, Notre Dame, IN 46556-5670, USA

† Electronic supplementary information (ESI) available: Additional crystallographic and MS data. CCDC reference number 739029. For ESI and crystallographic data in CIF or other electronic format see DOI: 10.1039/b913225b

for asymmetric catalysis, but these are correspondingly more expensive as well as being sterically hindered, and as such, unsuitable for the application we have in mind. Ercolani and co-workers monobenzylated diphenylphosphinomethane (dppm) and diphenylphosphinoethane (dppe) to make ligands of the form  $[\text{Ph}_2\text{P}(\text{CH}_2)_n\text{PPh}_2(\text{CH}_2\text{Ph})]^+ \text{X}^-$  ( $n = 1$  or  $2$ ;  $\text{X} = \text{Cl}, \text{Br}, \text{I}$ ). They reacted these ligands with anhydrous  $\text{CoX}_2$  and  $\text{NiX}_2$  to make tetrahedral zwitterionic complexes of the form  $\text{MX}_3\{\text{Ph}_2\text{P}(\text{CH}_2)_n\text{PPh}_2(\text{CH}_2\text{Ph})\}$ . The authors later extended their work to bisamine<sup>26</sup> and bisarsine<sup>27</sup> ligands. Berglund and Meek inadvertently prepared a related ligand when attempting to make  $\text{MeC}(\text{CH}_2\text{PPh}_2)_3$  from  $\text{MeC}(\text{CH}_2\text{Cl})_3$ ; their sodium diphenylphosphide was inadvertently partially hydrolyzed and so only two of the chlorides were replaced, forming a phosphetanium ion (Fig. 1).<sup>28</sup> This ligand can also be made rationally by deliberately adding only two equivalents of  $\text{NaPPh}_2$  to the reaction.<sup>29</sup> Their follow-up paper also describes the preparation of zwitterionic complexes and of the monocationic complex  $[\text{Au}(\text{L})\text{Cl}_3]\text{Cl}$  and the dicationic complex  $[\text{Pd}(\text{L})_2\text{Cl}_2](\text{ClO}_4)_2$ . Finally, in 1974, Taylor and co-workers made charged tungsten carbonyl complexes with *cis*- and *trans*-1,2-bis(diphenylphosphino)ethylene and bis(diphenylphosphino)acetylene,  $\text{W}(\text{CO})_5(\text{L})$ , which they methylated to form cationic  $[\text{W}(\text{CO})_5(\text{LMe})]^+$  complexes.<sup>30</sup> It appears that no one has employed ligands of this type for any application in the following 35 years.

An attractive test case for the efficacy of the charged phosphine/phosphonium ligand in ESI-MS would be any well-studied

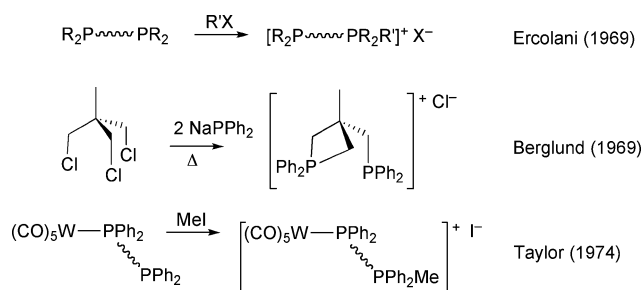
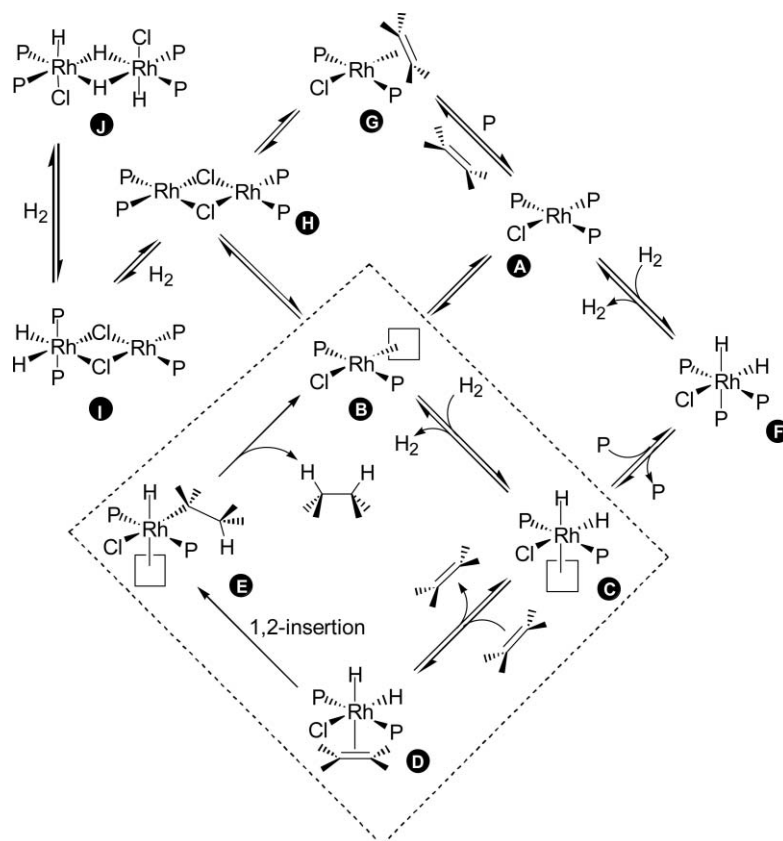


**Fig. 1** Published preparations of cationic phosphine/phosphonium ligands.

system involving a neutral catalyst with one or more phosphine ligands. Wilkinson's catalyst,  $\text{Rh}(\text{PPh}_3)_3\text{Cl}$ ,<sup>31</sup> is capable of effecting a wide range of transformations, including hydrogenation of isolated alkenes and alkynes.<sup>32</sup> Its popularity arose from its activity, tolerance of other functional groups, and its regio- and stereoselectivity.  $\text{Rh}(\text{PPh}_3)_3\text{Cl}$ -catalyzed hydrogenation has been examined in detail by kinetic<sup>33</sup> and  $^1\text{H}$ ,  $^{13}\text{C}$  and  $^{31}\text{P}$  NMR studies,<sup>34,35</sup> and the catalytic cycle has been textbook material for decades (Scheme 1).<sup>36–38</sup>

Despite its ubiquity, the reaction is rich in its solution-phase diversity and behaviour under different conditions.<sup>39</sup> Its complexity was nicely revealed using para-hydrogen induced polarisation NMR techniques,<sup>40</sup> including the identification of



**Scheme 1** The generally accepted catalytic cycle (involving species **B–E**) for olefin hydrogenation using Wilkinson's catalyst (**A**), and known off-cycle species (**F–J**).

a number of new solution complexes, including  $(\text{Ph}_3\text{P})_2\text{ClHRh}(\mu\text{-H})_2\text{RhCl}(\text{PPh}_3)_2$  (**J**).<sup>41</sup> Our goal was to replace at least one of the triphenylphosphine ligands with a charged analogue, and to see if ESI-MS was able to acquire a picture of the solution speciation consistent with what is already known; establishing the reliability of the approach is of course key to being able to apply it to new systems of interest.

## Experimental

All synthesis was performed under an inert atmosphere of  $\text{N}_2$  using standard glovebox or Schlenk procedures. Solvents were HPLC grade and purified on an MBraun solvent purification system (SPS). Chlorobenzene was distilled over  $\text{CaH}_2$  under  $\text{N}_2$ . Benzyl bromide was distilled and stored over molecular sieves at 3 °C. Cyclohexene was refluxed and distilled over maleic anhydride under  $\text{N}_2$ . All other chemicals were used as obtained (Aldrich, Oakville, Canada). Gases were obtained from Airgas (Calgary, Canada). NMR spectra were collected on either an AV-300 or AV-360 Bruker spectrometer. Internal references to  $\text{CHCl}_3$  ( $^1\text{H}$   $\delta$  = 7.26 ppm),  $\text{C}_6\text{D}_5\text{H}$  ( $^1\text{H}$   $\delta$  = 1.16 ppm) and external reference to 85% aqueous  $\text{H}_3\text{PO}_4$  ( $^{31}\text{P}$ ) were used as appropriate. The ligand exchange reaction was examined using  $^{31}\text{P}$  NMR by dissolving  $\text{RhCl}(\text{PPh}_3)_3$  (16 mg, 0.017 mmol) and  $4^+ \text{BF}_4^-$  (103 mg, 0.017 mmol) in 1 ml of chlorobenzene: $\text{C}_6\text{D}_6$  (4:1).

## Mass spectrometry

All mass spectra and gas phase experiments were performed on a Micromass Q-ToF *micro* hybrid quadrupole/time-of-flight mass spectrometer in positive ion mode using pneumatically-assisted electrospray ionization with a capillary voltage of 2900 V, source temperature of 100 °C and desolvation temperature of 180 °C. Solutions were run in chlorobenzene and introduced to the mass spectrometer by a syringe pump at a rate of 2 mL  $\text{h}^{-1}$ . Accurate mass data was obtained (after careful calibration) by locking to an internal standard, either tetraoctylammonium bromide  $[\text{C}_{32}\text{H}_{68}\text{N}]^+$  (466  $m/z$ ) or tetradodecylammonium bromide  $[\text{C}_{48}\text{H}_{100}\text{N}]^+$  (690  $m/z$ ), whichever was closer to the target mass. MS/MS experiments were conducted with argon in the collision cell. The appropriate peak was mass selected (usually with a broad enough window to accommodate the full isotope pattern, *i.e.*  $\sim 8 m/z$ ) and the selected ion fragmented at the stated voltage(s) in the argon-filled collision cell. Gas phase reactivity studies were conducted with the appropriate reactive gas in place of argon in the collision cell. All mass spectra were collected for a sufficiently long period to obtain a signal-to-noise ratio of at least 20:1; this ranged from a few seconds for ordinary mass spectra to 10 minutes for the gas phase reaction. ESI-MS spectra of the catalyst mixture were obtained by adding to 12 ml of chlorobenzene  $\text{RhCl}(\text{PPh}_3)_3$  (14 mg, 1.25 mmol  $\text{L}^{-1}$ ) and  $4^+ \text{BF}_4^-$  (2 mg, 0.28 mmol  $\text{L}^{-1}$ ) to give a bright orange solution. Hydrogen (99.995%) passed through the catalyst solution resulted in a peach-coloured solution in under 30 seconds.

**1-diphenylphosphino-1-benzylidiphenylphosphonium-methane bromide ( $1^+ \text{Br}^-$ ).** To a solution of 1,1-bisdiphenylphosphino-methane (510 mg, 1.33 mmol) in 15 ml dry,  $\text{N}_2$ -purged toluene at 0 °C was slowly added a dilute solution of benzyl bromide (227 mg, 157  $\mu\text{l}$ , 1.33 mmol) in 1 ml dry,  $\text{N}_2$ -purged toluene. The

clear, colourless solution was left to warm to room temperature overnight under  $\text{N}_2$ . The resulting white microcrystalline powder (330 mg, 45% yield) was retrieved *via* suction filtration, washed with cold toluene, and dried under high vacuum for 12 h. M.p.: 207-208 °C. ESI-MS (+ve): experimental: 475.1745  $m/z$  =  $[\text{P}_2\text{C}_{32}\text{H}_{29}]^+$ , calculated: 475.1744  $m/z$ .  $^1\text{H}$  NMR (300 MHz,  $\text{CDCl}_3$ ):  $\delta$  (ppm) = 4.28 (d,  $^1J_{\text{HP}}$  = 14, 2H), 4.96 (d,  $^1J_{\text{HP}}$  = 14, 2H), 7.09-7.79 (mm, 25H).  $^{31}\text{P}\{^1\text{H}\}$  NMR (360 MHz,  $\text{CDCl}_3$ ):  $\delta$  (ppm) = 26.07 (d,  $^2J_{\text{PP}}$  = 58,  $\text{P}^+$ ), -27.63 (d,  $^2J_{\text{PP}}$  = 58, P).

**1-diphenylphosphino-2-benzylidiphenylphosphonium-ethane bromide ( $2^+ \text{Br}^-$ ).** As for  $1^+ \text{Br}^-$ ; 1,2-bisdiphenylphosphinoethane (501 mg, 1.26 mmol) to benzyl bromide (215 mg, 150  $\mu\text{l}$ , 1.26 mmol) to give a white powder (319 mg, 45% yield). M.p.: 218-220 °C. ESI-MS (+ve): experimental: 489.1900  $m/z$  =  $[\text{P}_2\text{C}_{33}\text{H}_{31}]^+$ , calculated: 489.1901  $m/z$ .  $^1\text{H}$  NMR (300 MHz,  $\text{CDCl}_3$ ):  $\delta$  (ppm) = 2.17 (m, 2H), 3.04 (m, 2H), 5.06 (d,  $^1J_{\text{HP}}$  = 14, 2H), 6.93-7.77 (mm, 25H).  $^{31}\text{P}\{^1\text{H}\}$  NMR (360 MHz,  $\text{CDCl}_3$ ):  $\delta$  (ppm) = 28.24 (d,  $^3J_{\text{PP}}$  = 42,  $\text{P}^+$ ), -12.14 (d,  $^3J_{\text{PP}}$  = 42, P).

**1-diphenylphosphino-2-benzylidiphenylphosphonium-ethane tetraphenylborate ( $2^+ \text{BPh}_4^-$ ).** The tetraphenylborate salt of  $2^+$  was obtained by adding one equivalent of sodium tetraphenylborate (962 mg, 2.81 mmol) in 150 ml  $\text{N}_2$ -purged methanol to  $2^+ \text{Br}^-$  (1.599 g, 2.81 mmol) in 250 ml  $\text{N}_2$ -purged anhydrous ethanol. The resulting white precipitate (1.503 g, 66% yield) was isolated by suction filtration and dried under high vacuum.  $^{31}\text{P}$  NMR and positive-ion ESI-MS were identical to the bromide equivalent; the negative ion ESI-MS showed *no*  $\text{Br}^-$ , only  $\text{BPh}_4^-$  (318.17  $m/z$ ).

**1,1-bis(diphenylphosphino-methyl)-1-benzylidiphenylphosphonium-ethane bromide ( $3^+ \text{Br}^-$ ).** To a solution of 1,1,1-tris(diphenylphosphino-methyl)ethane (220 mg, 0.35 mmol) in 5 ml dry,  $\text{N}_2$ -purged toluene at 0 °C was slowly added a dilute solution of benzyl bromide (60 mg, 41  $\mu\text{l}$ , 0.35 mmol) in 1 ml dry,  $\text{N}_2$ -purged toluene. The clear, colourless solution was left to warm to room temperature overnight under  $\text{N}_2$ . The clear, colourless solution was reduced to half volume under high vacuum and 2 ml  $\text{N}_2$ -purged hexane is added. The resulting white powder (7 mg, 3% yield) was retrieved *via* suction filtration, washed with cold toluene, and dried under high vacuum for 12 h. M.p.: 106-109 °C. ESI-MS (+ve): experimental: 715.2814  $m/z$  =  $[\text{P}_3\text{C}_{48}\text{H}_{46}]^+$  calculated: 715.2813  $m/z$ .  $^1\text{H}$  NMR (300 MHz,  $\text{CDCl}_3$ ):  $\delta$  (ppm) = 1.00 (s, 3H), 2.03 (d,  $^1J_{\text{HP}}$  = 15, 2H), 2.69 (d,  $^1J_{\text{HP}}$  = 13, 2H), 3.97 (d,  $^1J_{\text{HP}}$  = 14, 2H), 4.84 (d,  $^1J_{\text{HP}}$  = 14, 2H), 6.81-8.26 (mm, 46H).  $^{31}\text{P}\{^1\text{H}\}$  NMR (360 MHz,  $\text{CDCl}_3$ ):  $\delta$  (ppm) = 23.76 ( $\text{P}^+$ ), -26.04 (P).

**1-diphenylphosphino-4-benzylidiphenylphosphonium-butane bromide ( $4^+ \text{Br}^-$ ).** As for  $1^+ \text{Br}^-$ ; 1,4-bisdiphenylphosphinobutane (500 mg, 1.17 mmol) to benzyl bromide (200 mg, 140  $\mu\text{l}$ , 1.17 mmol) to give a white powder (181 mg, 26% yield). M.p.: 156-158 °C. ESI-MS (+ve): experimental: 517.2209  $m/z$  =  $[\text{P}_2\text{C}_{35}\text{H}_{35}]^+$  calculated: 517.2214  $m/z$ .  $^1\text{H}$  NMR (300 MHz,  $\text{CDCl}_3$ ):  $\delta$  (ppm) = 1.50 (m, 4H), 1.92 (d,  $^3J_{\text{HH}}$  = 7, 2H), 3.12 (m, 2H), 4.90 (d,  $^1J_{\text{HP}}$  = 12, 2H), 6.97-7.76 (mm, 25H).  $^{31}\text{P}\{^1\text{H}\}$  NMR (360 MHz,  $\text{CDCl}_3$ ):  $\delta$  (ppm) = 27.86 ( $\text{P}^+$ ), -16.72 (P).

**1-diphenylphosphino-4-benzylidiphenylphosphonium-butane tetrafluoroborate ( $4^+ \text{BF}_4^-$ ) and hexafluorophosphate ( $4^+ \text{PF}_6^-$ ).** The tetrafluoroborate salt of  $4^+$  was obtained by stirring

2.5 equivalents of sodium tetrafluoroborate (108 mg, 0.98 mmol) with  $4^+$  Br $^-$  (235 mg, 0.39 mmol) in 20 ml N $_2$ -purged methanol. The methanol was removed by evaporation under high vacuum and N $_2$ -purged H $_2$ O is added to the resulting solid to dissolve the excess sodium tetrafluoroborate and the sodium bromide by-product. 1-diphenylphosphino-4-benzylidiphenylphosphonium-tetrafluoroborate was isolated from the resulting white slurry by suction filtration and dried under high vacuum to dryness (213 mg, 89% yield). The hexafluorophosphate salt was made in identical fashion in 73% yield. The  $^{31}\text{P}$  NMR and positive ion ESI-MS of both were identical to the bromide equivalent; the negative ion ESI-MS showed no Br $^-$  and only BF $_4^-$  (87.00  $m/z$ ) or PF $_6^-$  (144.96  $m/z$ ), respectively. Colourless, block-like single crystals of  $4^+$  PF $_6^-$  suitable for X-ray structural analysis were obtained by layering first a thin layer of cold 1-butanol followed by hexane over a concentrated dichloromethane solution of  $4^+$  PF $_6^-$  in a crystallisation tube in the glovebox.

**1-diphenylphosphino-6-benzylidiphenylphosphonium-hexane bromide ( $6^+$  Br $^-$ ).** As for  $1^+$  Br $^-$ ; 1,6-bisdiphenylphosphinohexane (100 mg, 0.22 mmol) to benzyl bromide (40 mg, 26  $\mu\text{l}$ , 0.22 mmol) to give a white powder (28 mg, 20% yield). M.p.: 132–134  $^\circ\text{C}$ . ESI-MS (+ve): experimental: 545.2527  $m/z$  = [P $_2$ C $_{37}$ H $_{39}$ ] $^+$  calculated: 545.2527  $m/z$ .  $^1\text{H}$  NMR (300 MHz, CDCl $_3$ ):  $\delta$  (ppm) = 1.26 (m, 8H), 1.85 (m, 2H), 3.11 (m, 2H), 4.85 (d,  $^3J_{\text{HP}} = 15$ , 2H), 6.95–7.73 (m, 25H).  $^{31}\text{P}\{^1\text{H}\}$  NMR (360 MHz, CDCl $_3$ ):  $\delta$  = 27.93 (P $^+$ ), 15.92 (P).

## Results and discussion

### The ligands

The phosphine/phosphonium ligands [Ph $_2$ P(CH $_2$ ) $_n$ PPh $_2$ Bn] $^+$  Br $^-$  ( $n = 1, 2, 4, 6$ ; Bn = benzyl; cations referred to as  $1^+$ ,  $2^+$ ,  $4^+$ ,  $6^+$ ) and [MeC(CH $_2$ PPh $_2$ ) $_2$ (CH $_2$ PPh $_2$ Bn)] $^+$  Br $^-$  ( $3^+$ ) were made from benzyl bromide and the corresponding commercially available bis- and trisphosphines (Fig. 2). The preparation is similar to that originally employed by Ercolani *et al.*<sup>27</sup> To improve the solubility of the ligands in less polar solvents and to remove the potential complication of the Br $^-$  anion (which can act as a ligand, *vide infra*),  $4^+$  Br $^-$  was metathesized with sodium tetrafluoroborate to make  $4^+$  BF $_4^-$ .

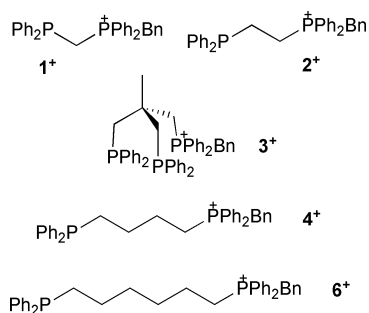


**Fig. 2** The five cationic ligands used in this study; the counterion was Br $^-$ , BF $_4^-$  or PF $_6^-$ .

The Br $^-$  and BF $_4^-$  salts did not provide single crystals, but the hexafluorophosphate salt of  $4^+$  did and was structurally characterized (Fig. 3). The structure of the cation and anion is

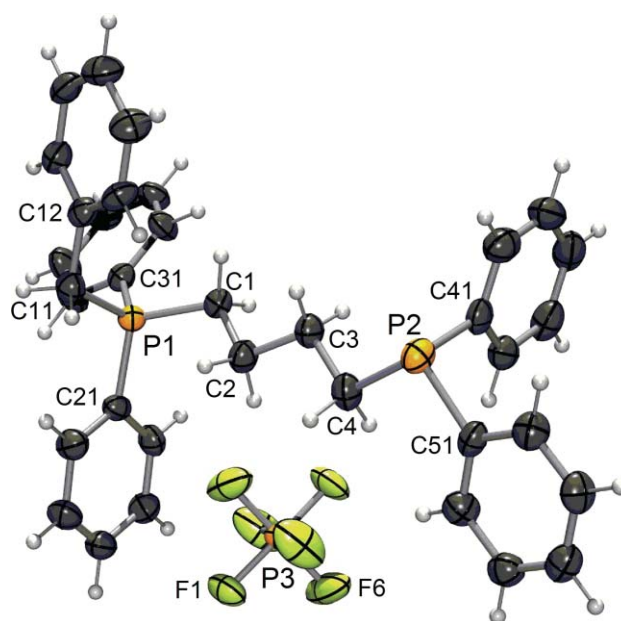


**Fig. 3** Single crystal X-ray structure of [Ph $_2$ P(CH $_2$ ) $_4$ PPh $_2$ Bn] $^+$  [PF $_6$ ] $^-$ . Selected bond distances: P(1)–C(31) 1.792(3) Å; P(1)–C(21) 1.794(3) Å; P(1)–C(1) 1.803(3) Å; P(1)–C(11) 1.813(3) Å; P(2)–C(41) 1.834(3) Å; P(2)–C(4) 1.838(3) Å; P(2)–C(51) 1.840(3) Å. Selected bond angles: C(31)–P(1)–C(21) 109.80(12) $^\circ$ ; C(31)–P(1)–C(1) 108.86(13) $^\circ$ ; C(21)–P(1)–C(1) 110.62(12) $^\circ$ ; C(31)–P(1)–C(11) 111.57(13) $^\circ$ ; C(21)–P(1)–C(11) 107.47(13) $^\circ$ ; C(1)–P(1)–C(11) 108.53(13) $^\circ$ ; C(41)–P(2)–C(4) 100.77(13) $^\circ$ ; C(41)–P(2)–C(51) 99.43(13) $^\circ$ ; C(4)–P(2)–C(51) 103.58(13) $^\circ$ . Image drawn with ellipsoids at 70% probability using ORTEP-3.<sup>44</sup>

as expected. The P–C bond distances about P1 (phosphonium) are slightly shorter than those around P2 (phosphine). The C–P–C bond angles around P1 are more close to the ideal tetrahedral angle, in the range of 107.47(13) to 111.57(13) $^\circ$ , while those about P2 are more constrained and have moved to smaller angles, in the range of 99.43(13) to 103.58(13) $^\circ$ . The bond distances and angles about the phosphine in  $4^+$  PF $_6^-$  are very similar to those in the parent disphosphine 1,4-bis(diphenylphosphino)butane,<sup>42</sup> and in the diphenylalkyl phosphine Ph $_2$ P(CH $_2$ ) $_n$ Br.<sup>43</sup> P–C bond lengths are within 0.01 Å between all three structures and the sum of the three C–P–C angles are 304.05 $^\circ$  for 1,4-bis(diphenylphosphino)butane, 303.78 $^\circ$  for Ph $_2$ P(CH $_2$ ) $_n$ Br and (also) 303.78 $^\circ$  for  $4^+$  PF $_6^-$ . Further confirmation that the phosphine is essentially chemically unaffected by the alkylation of the other phosphine comes from  $^{31}\text{P}$  NMR; the chemical shift in CDCl $_3$  for the phosphine in 1,4-bis(diphenylphosphino)butane is –15.6 ppm, and –16.7 ppm in  $4^+$  Br $^-$ .

Addition of one equivalent of  $4^+$  BF $_4^-$  to one equivalent of RhCl(PPh $_3$ ) $_3$  in chlorobenzene:C $_6$ D $_6$  (4:1) revealed that  $4^+$  bound more strongly to Rh than PPh $_3$ , as the  $^{31}\text{P}$  NMR signal corresponding to the uncoordinated phosphine of  $4^+$  entirely disappeared to be replaced by signals indicating the phosphine of  $4^+$  had bound to rhodium. The spectrum was complicated by the fact that substitution could occur *cis* or *trans* to the chloride, and that further complexity was added by double substitution (also with *cis* and *trans* isomers). Free triphenylphosphine was observed in the appropriate proportion. Replacement of one phenyl group

on phosphine with an alkyl group makes the ligand a stronger base and a better donor, hence the efficiency of  $4^+$  in replacing  $\text{PPh}_3$ .

### ESI-MS analysis

Sub-stoichiometric amounts of the charged ligands were used for ESI-MS analysis of the catalyst solutions, approximately a 1:5 ratio of ligand: $\text{Rh}(\text{PPh}_3)_3\text{Cl}$ , thus essentially just “doping” the system with the ligand. Why? Multiply charged species can cause complications in ESI-MS if the mass-to-charge ratio gets too low, as charge-reduction processes can occur during the electrospray ionisation process (in this case, simple dissociation of a ligand due to Coulombic repulsion). Doping makes the synthesis simple and efficient (less of the custom ligand is used), and finally, the concentration of the ligand can be selected for optimal ESI-MS performance (usually very low) while still running the catalysis under “real” conditions (normal catalyst concentration). Ethanol, ethanol/benzene (1:1) and chlorobenzene were all tried as solvents; formation of phosphine oxide was worst in ethanol, and signal intensity was somewhat compromised in ethanol/benzene, so chlorobenzene (b.p.  $131^\circ\text{C}$ ) was settled on as a good compromise solvent, as it is volatile enough and polar enough to support the electrospray ionization process<sup>2</sup> while oxidation of the ligand was minimized.

The first experiment examined a mixture of  $\text{Rh}(\text{PPh}_3)_3\text{Cl}$  and  $2^+ \text{Br}^-$  (5:1), which immediately revealed difficulties with both this particular cationic ligand and its bromide counterion. As expected, the ion  $[\text{Rh}(\text{PPh}_3)_2(2^+)\text{Cl}]^+$  was detected (where  $2^+ \text{Br}^-$  has displaced one equivalent of  $\text{PPh}_3$ ), along with the dimeric species  $[\text{Rh}_2(\mu\text{-Cl})_2(\text{PPh}_3)_3(2^+)]^+$ . In addition, however, a certain degree of halide exchange occurred, resulting in the appearance of Br-containing ions, and the  $[\text{Rh}(\text{dppe})_2]^+$  cation was also observed at  $899.2 m/z$  (presumably generated *via* dealkylation of  $2^+ \text{Br}^-$ , as dppe is undetectable by  $^{31}\text{P}$  NMR in the sample of  $2^+ \text{Br}^-$ ). Two changes were therefore made before proceeding further; one to lengthen the alkyl chain linking the two phosphorus atoms from  $(\text{CH}_2)_2$  to  $(\text{CH}_2)_4$  to negate the chelate effect, and another to replace the bromide counterion with the relatively non-coordinating tetrafluoroborate ion (i.e.  $4^+ \text{BF}_4^-$  was used instead of  $2^+ \text{Br}^-$ ).

### Analysis of solution speciation: $\text{RhCl}(\text{PPh}_3)_3 + 4^+ \text{BF}_4^-$ in chlorobenzene

Addition of  $4^+ \text{BF}_4^-$  to  $\text{RhCl}(\text{PPh}_3)_3$  (1:5) in chlorobenzene reveals a number of peaks (Fig. 4), but all are consistent with the known solution behaviour of the catalyst (and the spectrum is simpler with the Br-containing species and  $[\text{Rh}(\text{bisphosphine})_2]^+$  now absent). The phosphine ligands on the complex are quite labile,<sup>45</sup> and stirring the complex in benzene slowly generates the rather insoluble dimeric  $\text{Rh}_2(\mu\text{-Cl})_2(\text{PPh}_3)_4$ , “Wilkinson’s dimer”.<sup>32</sup> In keeping with these facts, the ESI-MS spectrum reveals species in which either one or two  $\text{PPh}_3$  ligands of the dimer or the monomer have been replaced by  $4^+$ . Additionally, free  $4^+$  is observed as well as oxidised  $4^+$  ( $4\text{O}^+$ ; phosphine oxides are often observed even when stringent precautions are taken).<sup>46</sup> A small amount of the bis-substituted complex is observed accompanied by the  $\text{BF}_4^-$  counterion, thus appearing as a monocation  $[\text{RhCl}(\text{PPh}_3)_2(4^+)_2 + \text{BF}_4]^+$  at  $1521 m/z$ . A small amount of  $[\text{Rh}(\text{PPh}_3)_3]^+$  is observed,

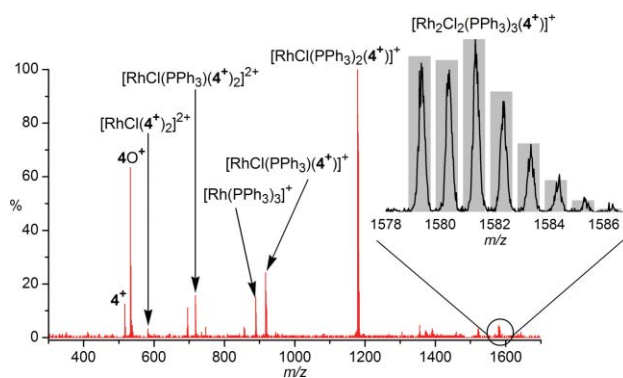


**Fig. 4** Positive-ion ESI-MS of  $\text{RhCl}(\text{PPh}_3)_3 + 4^+ \text{BF}_4^-$  in chlorobenzene at a cone voltage setting of 10 V. Inset shows the isotope pattern match for  $[\text{Rh}_2\text{Cl}_2(\text{PPh}_3)_3(4^+)]^+$  (calculated pattern in grey bars).

presumably generated *via* chloride loss from  $\text{RhCl}(\text{PPh}_3)_3$  (halide loss is a well-known ionization process in ESI-MS).<sup>47</sup>

The appearance of  $[\text{RhCl}(4^+)_2]^{2+}$  and  $[\text{RhCl}(\text{PPh}_3)(4^+)]^+$ , highly reactive B-type three-coordinate species (see Scheme 1), is the result of fragmentation of  $[\text{RhCl}(\text{PPh}_3)_2(4^+)]^{2+}$  and  $[\text{RhCl}(\text{PPh}_3)_3(4^+)]^+$  (A-type species). Even at very low cone voltage, phosphine loss occurs, but it is clear that the process is occurring primarily in the gas phase, as revealed by monitoring relative ion intensity as a function of cone voltage (see Fig. 5).

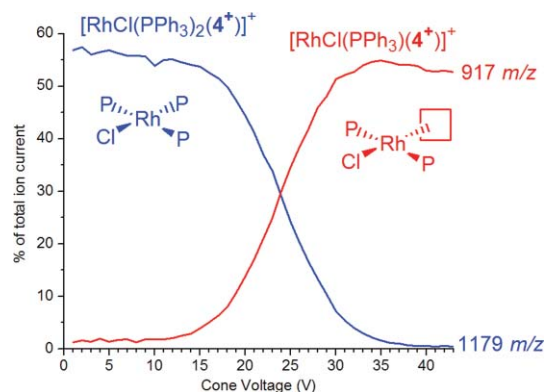


**Fig. 5** Intensity of  $[\text{RhCl}(\text{PPh}_3)_2(4^+)]^+$  (precursor) and  $[\text{RhCl}(\text{PPh}_3)(4^+)]^+$  (product) ions as a proportion of total ion current as cone voltage is increased.

Both  $[\text{RhCl}(\text{PPh}_3)(4^+)]^{2+}$  and  $[\text{RhCl}(\text{PPh}_3)_2(4^+)]^+$  readily lose a phosphine ligand; Fig. 5 indicates that the latter always loses  $\text{PPh}_3$ , but the former loses *either*  $\text{PPh}_3$  or  $4^+$  in a competitive process (see supporting information). While  $4^+$  is a more tenacious ligand, the presence of two positively charged ligands results in Coulombic repulsion between them and hence in the gas phase the Rh-P bond is effectively weakened. Note in Fig. 6 how the maximum intensity of  $[\text{RhCl}(4^+)_2]^{2+}$  is lower than that of  $[\text{RhCl}(\text{PPh}_3)(4^+)]^+$ , because some of the latter is eliminating  $4^+$  instead of  $\text{PPh}_3$ . Plotted on the same graph is  $[\text{Rh}_2\text{Cl}_2(\text{PPh}_3)_3(4^+)]^+$ , which is clearly less labile, staying intact as the cone voltage is increased.

The fragility of the  $\text{RhClP}_3$  (A) species is consistent with what is already known about the chemistry of this complex, which is known to readily dissociate a phosphine ligand. It does reveal an important consideration when running ESI-MS of complexes

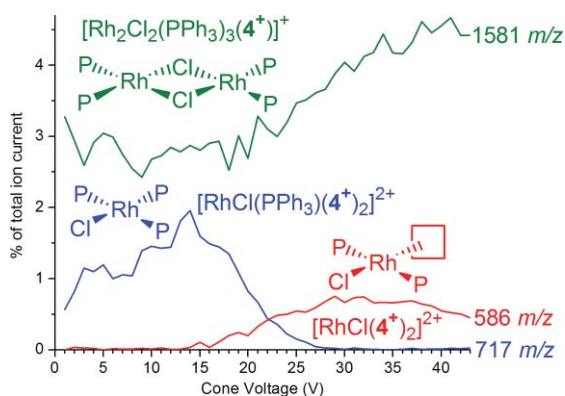


**Fig. 6** Intensity of  $[\text{RhCl}(\text{PPh}_3)_2(4^+)]^+$  (precursor) and  $[\text{RhCl}(4^+)]_2^{2+}$  (product) ions as a proportion of total ion current as cone voltage is increased. The intensity of the  $[\text{Rh}_2\text{Cl}_2(\text{PPh}_3)_3(4^+)]^+$  ion is also plotted.

of this type, in that the cone voltage (or whatever parameter controls collision induced dissociation in the source) must be kept as low as possible. This precaution is generally an easy one to take, since organometallic complexes rarely need the aggressive desolvating that polar organic molecules require for clean analysis, but there is still a trade-off: total ion current increases linearly with cone voltage (at low cone voltage; see supporting information†), because ion transmission from the atmospheric pressure source to the high vacuum of the mass analyser(s) is greatly improved by accelerating the ion through the intermediate region.

As a result, although the lowest cone voltages tend to give the most accurate representation of the solution speciation, their signal-to-noise is also usually the lowest. We tend to use 20 V as a default value (values of 40–50 V are more typical for polar organic molecules): minimal fragmentation even for very labile complexes, but reasonably high response. In this study, because of the unusual lability of the complexes under study, we typically used 10 V and collected spectra for a longer period than usual (minutes rather than seconds). Note that while ESI-MS analysis can be made quantitative through calibration, in this work we have not attempted to provide more than a qualitative analysis of speciation. Peak intensities do vary considerably even for equimolar amounts of compounds carrying the same charge, due to the degree to which a particular ion is “surface-active” (*i.e.* least prone to ion-pair and least solvated; such ions are over-represented in the mass spectrum).<sup>48</sup> Despite the fact that the relative intensities of different ions do not necessarily accurately represent their relative concentrations, it is possible to say something more concrete about their relative abundances because the detector response is essentially linear at all but very high concentrations. So *changes* in intensity are meaningful, even though the absolute intensity may misrepresent the actual concentration.

In comparison to **A**, the dimer  $[\text{Rh}_2\text{Cl}_2(\text{PPh}_3)_3(4^+)]^+$  (**H**) is remarkably robust and under acceleration into argon atoms in the collision cell (“collision induced dissociation”, or CID), does not fragment at all *via* loss of phosphine. In keeping with its known chemistry, it instead splits in two symmetrically, breaking the two Rh–Cl bonds and forming  $[\text{RhCl}(\text{PPh}_3)_2(4^+)]^+$  (**B**) *i.e.* losing  $\text{RhCl}(\text{PPh}_3)_2$  (**B**). The resulting MS/MS spectrum is shown in the supporting information. The process **H** → **2B** is the reverse of the reaction thought to generate **H** in solution.

### Analysis of solution speciation: $\text{RhCl}(\text{PPh}_3)_3 + 4^+ \text{BF}_4^- + \text{H}_2$ in chlorobenzene

When hydrogen gas is bubbled through the chlorobenzene solution, an immediate change in the ESI-MS is observed, though at first glance the change is not especially dramatic. Most noticeable is that more of the three-coordinate species  $[\text{RhCl}(\text{PPh}_3)_2(4^+)]^+$  (**B**) appears (see Table 1, and the supporting information† for the spectrum), even at a cone voltage of 10 V. However, a close inspection of the isotope patterns of the major peaks indicates that a reaction with  $\text{H}_2$  has also occurred. Despite overlap between the isotope patterns for the unreacted and  $+\text{H}_2$  species, the relative proportions of each can still be modelled with a good degree of accuracy (especially for the more abundant species; see Fig. 7).

The speciation does not, of course, tell us by which path the reactions occurred; for example, the formation of  $\text{RhCl}(\text{PPh}_3)_3\text{H}_2$  (**F**) from  $\text{RhCl}(\text{PPh}_3)_3$  (**A**) is thought to proceed *via*  $\text{RhCl}(\text{PPh}_3)_2$  (**B**) and  $\text{RhCl}(\text{PPh}_3)_2\text{H}_2$  (**C**).<sup>33</sup> The solution stability of **C** appears to be very low; clearly, this five-coordinate species is sufficiently reactive that it cannot be detected. Interestingly, its gas phase stability is also low, from MS/MS evidence. **C** can be “prepared” in the gas phase by dissociating a phosphine ligand from **F**, the six-coordinate  $[\text{RhCl}(\text{PPh}_3)_2(4^+)\text{H}_2]^+$ . The fragmentation of **F** by CID results first in loss of  $\text{PPh}_3$ , then of  $\text{H}_2$ . No sign of the inverse order is observed, *i.e.* loss of  $\text{H}_2$  then  $\text{PPh}_3$  (Fig. 8). However, the collision energy needs to be selected with care; at 6 V, the five-coordinate  $[\text{RhCl}(\text{PPh}_3)_2(4^+)\text{H}_2]^+$  (loss of  $\text{PPh}_3$  only) can be observed at approximately the same intensity as the three-coordinate  $[\text{RhCl}(\text{PPh}_3)_2(4^+)]^+$  (loss of  $\text{PPh}_3$  and  $\text{H}_2$ ). At lower energy, neither fragmentation occurs to any extent, and at higher energy, only the three-coordinate fragment ion  $[\text{RhCl}(\text{PPh}_3)_2(4^+)]^+$  is observed, suggesting that  $\text{H}_2$  loss from  $[\text{RhCl}(\text{PPh}_3)_2(4^+)\text{H}_2]^+$  is very facile. Such behaviour is unusual, because more typically loss of a ligand from a transition metal complex in the gas phase results in the remaining ligands being more tightly bound and correspondingly more difficult to remove.<sup>49,50</sup>

The increased amount of  $[\text{RhCl}(\text{PPh}_3)_2(4^+)]^+$  (**B**) present in the hydrogenated spectrum (supporting information†) is significant, because we know it is present as a fragment—in the  $\text{H}_2$ -free spectrum, of  $[\text{RhCl}(\text{PPh}_3)_2(4^+)]^+$  (**A**)—and given that **A** is present at barely 10% abundance, we would not expect to see much of any **B**. Instead, even at the lowest cone voltages, it is present in substantial quantities compared to the non-hydrogenated spectrum (see Fig. 9):

The six-coordinate species begins fragmenting at a cone voltage of 10 V, and loses  $\text{PPh}_3$  (and  $\text{H}_2$ ) at a cone voltage approximately 5 V lower than  $[\text{RhCl}(\text{PPh}_3)_2(4^+)]^+$  loses  $\text{PPh}_3$  (see Fig. 5). This observation implies that the  $\text{PPh}_3$  is less tightly bound in **F** than in **A**, consistent with NMR results that give phosphine dissociation rates from **F** as  $400 \text{ s}^{-1}$  compared to  $0.31 \text{ s}^{-1}$  for **A**.<sup>35</sup> The most interesting aspect of Figure 11, however, is the fact that the three-coordinate species makes up approximately 15% of the ion current even at the lowest values of cone voltage (the *additional*  $[\text{RhCl}(\text{PPh}_3)_2(4^+)]^+$  that appears after 10 V comes from fragmentation of  $[\text{RhCl}(\text{PPh}_3)_2(4^+)\text{H}_2]^+$ ). This observation suggests that the three-coordinate species is generated from the dissociation of some other, very weakly coordinated ligand that is not present in the non-hydrogenated sample. The only ligand possible is hydrogen, presumably as the five-coordinate dihydride

**Table 1** Solution speciation by positive-ion ESI-MS (10 V) at various stages in the catalytic hydrogenation of cyclohexene using Wilkinson's catalyst and  $4^+ \text{BF}_4^-$  in chlorobenzene

Species	Cycle	Identity	$m/z$	Intensity before $\text{H}_2$ addition	Intensity after $\text{H}_2$ addition	Intensity after cyclohexene addition
Free ligand		$[4^+]^+$	517.2	13%	13%	4%
Oxidised ligand		$[4\text{O}^+]^+$	533.2	63%	55%	34%
RhCIP <sub>2</sub>	B	$[\text{RhCl}(4^+)_2]^{2+}$	586.2	11%	3%	<1%
	B	$[\text{RhCl}(\text{PPh}_3)(4^+)]^+$	917.2	24%	100%	6%
RhP <sub>3</sub> <sup>+</sup>		$[\text{Rh}(\text{PPh}_3)_3]^+$	889.2	15%	8%	30%
RhCIP <sub>3</sub>	A	$[\text{RhCl}(\text{PPh}_3)(4^+)_2]^{2+}$	717.2	16%	9%	<1%
	F	$[\text{RhCl}(\text{PPh}_3)(4^+)_2\text{H}_2]^{2+}$	718.2	—	3%	<1%
	A	$[\text{RhCl}(\text{PPh}_3)_2(4^+)]^+$	1179.3	100%	10%	100%
	F	$[\text{RhCl}(\text{PPh}_3)_2(4^+)\text{H}_2]^+$	1181.3	—	77%	<1%
	A	$[\text{RhCl}(\text{PPh}_3)(4^+) + \text{BF}_4]^+$	1521.4	4%	<1%	2%
	F	$[\text{RhCl}(\text{PPh}_3)(4^+)_2\text{H}_2 + \text{BF}_4]^+$	1523.4	—	2%	<1%
Rh <sub>2</sub> Cl <sub>2</sub> P <sub>4</sub>	H	$[\text{Rh}_2\text{Cl}_2(\text{PPh}_3)_3(4^+)]^+$	1581.2	6%	2%	3%
	I	$[\text{Rh}_2\text{Cl}_2(\text{PPh}_3)_3(4^+)\text{H}_2]^+$	1583.2	—	2%	<1%
	J	$[\text{Rh}_2\text{Cl}_2(\text{PPh}_3)_3(4^+)\text{H}_4]^+$	1585.2	—	<1%	<1%

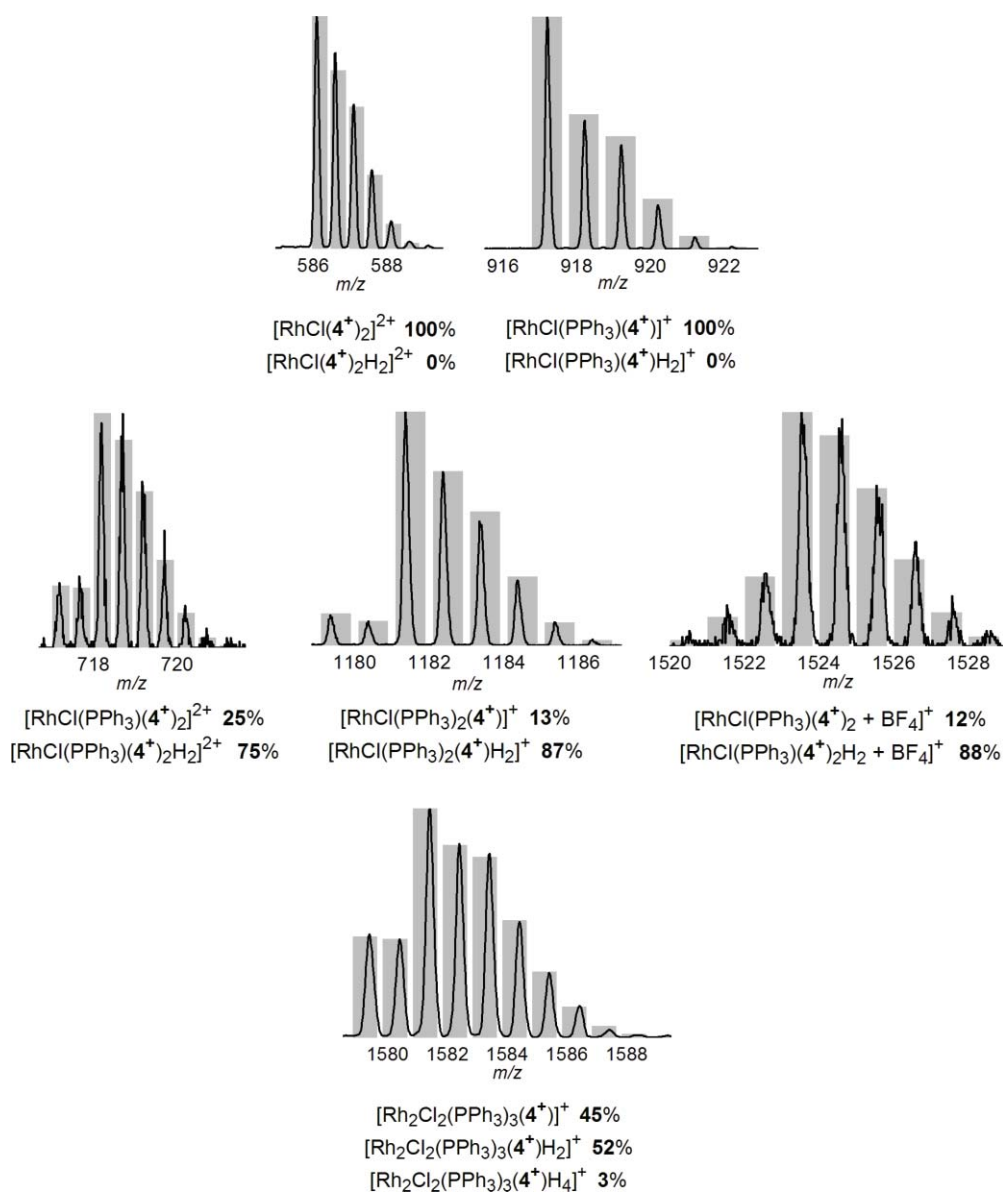


**Fig. 7** Isotope patterns for key species; the calculated values (grey bars) combine the isotope patterns for the listed species in the proportions given (which provide the best possible fit for the data). Note how the dications have peaks separated by  $0.5 m/z$ . Top row: RhCIP<sub>2</sub> (**B**) species; middle row: RhCIP<sub>3</sub> overlapping with RhCIP<sub>3</sub>H<sub>2</sub> (**A** and **F**) species; bottom row: Rh<sub>2</sub>Cl<sub>2</sub>P<sub>4</sub> overlapping with Rh<sub>2</sub>Cl<sub>2</sub>P<sub>4</sub>H<sub>2</sub> and Rh<sub>2</sub>Cl<sub>2</sub>P<sub>4</sub>H<sub>4</sub> (**H**, **I** and **J**) species.

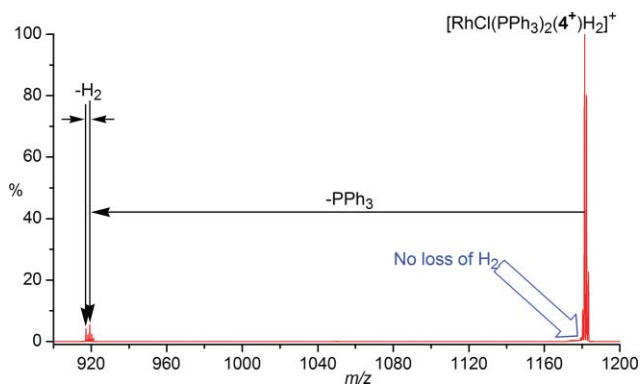


**Fig. 8** ESI-MS/MS of  $[\text{RhCl}(\text{PPh}_3)_2(4^+)\text{H}_2]^+$ . No loss of  $\text{H}_2$  is observed prior to loss of  $\text{PPh}_3$ .

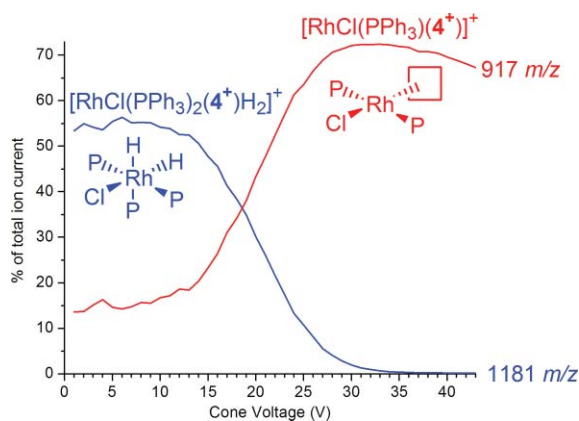


**Fig. 9** Intensity of  $[\text{RhCl}(\text{PPh}_3)_2(4^+)\text{H}_2]^+$  (**F**) and  $[\text{RhCl}(\text{PPh}_3)(4^+)]^+$  (**B**) ions as a proportion of total ion current as cone voltage is increased.

$[\text{RhCl}(\text{PPh}_3)_2(4^+)\text{H}_2]^+$  (**C**). We see none of this species in the mass spectrum (Fig. 9), but given how rapidly it decomposes in the gas phase (Fig. 8), this result is perhaps unsurprising.

The six-coordinate octahedral  $\text{Rh}^{\text{III}}$  species **F** are sufficiently stable that little **A** remains in the solution after  $\text{H}_2$  addition, consistent with the importance of **F** as a resting state.<sup>51</sup> The dimeric  $\text{Rh}_2\text{Cl}_2\text{P}_4$  compound (**H**) also lessens in intensity by about 50%, with a proportional amount of  $\text{Rh}_2\text{Cl}_2\text{P}_4\text{H}_2$  (**I**) and a small amount of  $\text{Rh}_2\text{Cl}_2\text{P}_4\text{H}_4$  (**J**) appearing in the spectrum.

#### Analysis of solution speciation: $\text{RhCl}(\text{PPh}_3)_3 + 4^+ \text{BF}_4^- +$ cyclohexene in chlorobenzene

No simple compounds incorporating the alkene were observed upon addition of cyclohexene, *i.e.* no  $[\text{RhCl}(\text{PPh}_3)(4^+)(\text{C}_6\text{H}_{10})]^+$  (**G**). Instead, a number of ions were detected that incorporated a ligand 2  $m/z$  less than expected for the alkene:  $[\text{RhCl}(\text{PPh}_3)(4^+)(\text{C}_6\text{H}_8)]^+$  (997.2  $m/z$ ),  $[\text{RhCl}(4^+)(\text{C}_6\text{H}_8)]^+$  (735.2  $m/z$ ) and  $[\text{Rh}(\text{PPh}_3)_2(\text{C}_6\text{H}_8)]^+$  (707.2  $m/z$ ). Analogous species were observed when 1-hexene was used instead of cyclohexene. MS/MS of the 997.3  $m/z$  peak revealed that the  $\text{C}_6\text{H}_8$  was more strongly bound to the Rh than either  $\text{PPh}_3$  or  $4^+$ , as CID produced only a small amount of the  $[\text{RhCl}(\text{PPh}_3)(4^+)]^+$  product ion, instead producing mostly  $[\text{RhCl}(4^+)(\text{C}_6\text{H}_8)]^+$  and free  $4^+$  (see supporting information). The source of the  $\text{C}_6\text{H}_8$  (or  $\text{C}_6\text{H}_{10}$  in the case of 1-hexene) ligand is most likely to be 1,4-cyclohexadiene; any 1,3-

cyclohexadiene is removed during purification of the cyclohexene (distillation from maleic anhydride removes any conjugated dienes through a Diels–Alder reaction). We tested this assumption by reacting both 1,4- and 1,3-cyclohexadiene directly with the doped catalyst solution, and both rapidly formed the 707 and 735  $m/z$  species, both of which had identical MS/MS fragmentation patterns as observed in the same species seen in the original spectrum with no added diene. Interestingly, while the two peaks appeared immediately in the case of the 1,3-cyclohexadiene, they grew in over the space of a few minutes for the 1,4-cyclohexadiene. We suggest that this is most likely due to isomerisation of the 1,4-diene to the 1,3-diene, the latter being the probable catalyst poison. We are investigating these reactions in more detail. Potentially chelating (*e.g.* 1,4-cyclohexadiene) or conjugated dienes (*e.g.* 1,3-cyclohexadiene) are known to be very difficult to reduce at 1 atm of  $\text{H}_2$  (though are reduced at 60 atm), probably due to the formation of a strong complex.<sup>52</sup>

#### Analysis of solution speciation: $\text{RhCl}(\text{PPh}_3)_3 + 4^+ \text{BF}_4^- + \text{H}_2 +$ cyclohexene in chlorobenzene

The rate of olefin hydrogenation varies widely depending on the sterics (cyclohexene is hydrogenated 50× faster than 1-methylcyclohexene) and electronics of the olefin. Addition of cyclohexene to a continually hydrogen-saturated chlorobenzene solution of  $\text{RhCl}(\text{PPh}_3)_3$  and  $4^+ \text{BF}_4^-$  resulted in significant changes to the solution speciation, most notably the disappearance of all **F**-type species (*i.e.* no  $\text{RhClP}_3\text{H}_2$ ; speciation for the different experiments are summarized in Table 1). This observation is in keeping with the known pathway for formation of **F** from **A** via **B** and **C**; the excess alkene present will presumably trap any **C** present to form **D**.

Despite the change in speciation, no new alkene-containing species were observed *e.g.*  $[\text{RhCl}(\text{PPh}_3)(4^+)(\text{alkene})\text{H}_2]^+$  (**D**), though the same diene-containing species were observed as when cyclohexene alone was added. Bubbling ethylene through the hydrogen-saturated solution resulted in the appearance of a small amount (~2%) of  $[\text{RhCl}(\text{PPh}_3)(4^+)(\text{H}_2\text{C}=\text{CH}_2)]^+$  (**G**). The disappearance of **F**-type species was not seen as for the other alkenes, perhaps due to the relatively low effective concentration of the alkene.

#### Gas-phase reactivity: propylene

Gas phase reactivity studies may be implemented even on a barely-modified commercial ESI tandem mass spectrometer, and there are various points at which reactive gases can be introduced: in the source or in the collision cell (replacing the inert gas used for fragmentation) of a tandem instrument,<sup>53</sup> or in the cell of a trapping mass spectrometer.<sup>54</sup>  $[\text{RhCl}(\text{PPh}_3)_2(4^+)]^+$  (**A**) and  $[\text{RhCl}(\text{PPh}_3)(4^+)]^+$  (**B**) were selected (in separate experiments) using the quadrupole mass analyser and allowed to interact with propylene in the gas phase in the collision cell. As expected, the four-coordinate species **A** failed to react at all under these conditions, whereas the unsaturated three-coordinate species **B** readily reacted with  $\text{C}_3\text{H}_6$  to form the +42  $m/z$  species  $[\text{RhCl}(\text{PPh}_3)(4^+)(\text{C}_3\text{H}_6)]^+$ , the equivalent of the off-cycle species **G** (Fig. 10). The efficiency of formation was not high (the product ion is detected at ~0.6% of the intensity of the precursor ion), but

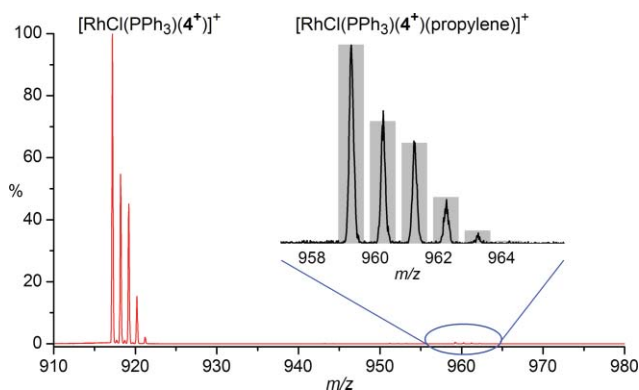


**Fig. 10** Gas phase reaction between  $[\text{RhCl}(\text{PPh}_3)(4^+)]^+$  and propylene. Most of the selected ion passes through the collision cell unchanged (917.2) but approximately 0.6% reacts with propylene (inset).

the identity of the product is not in doubt (see inset). The low gas-phase reactivity is in keeping with the observed low solution reactivity.

Reaction of  $[\text{RhCl}(\text{PPh}_3)_2(4^+)]^+$  (A) and  $[\text{RhCl}(\text{PPh}_3)(4^+)]^+$  (B) with  $\text{H}_2$  in the collision cell under the same conditions as for propylene results in no discernible reactivity for either ion; however, gas phase reactions with hydrogen are often inefficient, even for highly exothermic reactions with barely ligated ions.<sup>55</sup> There are ways in which to increase the number of collisions, and Chen *et al.* have illustrated the use of octopole<sup>56–58</sup> and even 24-pole ion guides<sup>14</sup> to increase the pressure of reactive gas and hence the efficiency of gas phase reactions with organometallic species. While  $[\text{RhCl}(\text{PPh}_3)_2(4^+)\text{H}_2]^+$  (C) can be made in the gas phase by carefully fragmenting  $[\text{RhCl}(\text{PPh}_3)_2(4^+)\text{H}_2]^+$  (F), insufficient amounts could be isolated by the quadrupole to allow for gas phase reactivity studies to be performed in the collision cell.

## Conclusions

Mono-alkylation of bisphosphines is a straightforward route to charged phosphine/phosphonium ligands from commercially available precursors. The ligands confer their charge to the complex to which they are bound, allowing their facile detection by ESI-MS. If the complexes in question are labile, there is no requirement for stoichiometric quantities of the ligand to be used; instead, the ligand may simply be *doped* into the system in a proportion that matches the (usually) differing concentration requirements of catalytic activity (typically millimolar) and ESI-MS performance (typically sub-millimolar). Good quality information on solution speciation may be thereby obtained directly from reaction solutions, though the facile fragmentation of labile complexes does mean that attention must be paid to the ESI conditions to ensure that the spectrum gives an accurate representation of the solution. Analysis of olefin hydrogenation by Wilkinson's catalyst using this method revealed that all *off*-cycle species could be rapidly identified, along with diene-derived catalyst poisons. Unsaturated, catalytically-active  $\text{RhClP}_2$  and  $\text{RhClP}_2\text{H}_2$  could be generated in the gas phase through loss of a phosphine ligand from  $\text{RhClP}_3$  or  $\text{RhClP}_3\text{H}_2$  respectively *via* collision-induced dissociation, revealing the ease with which ESI-MS can be used for the gas-phase synthesis of probable reactive

intermediates.  $\text{RhClP}_2$  was found to react in the gas phase with propylene to form  $\text{RhClP}_2(\text{propylene})$ .

## Acknowledgements

JSM thanks the Natural Sciences and Engineering Research Council (NSERC) of Canada, the Canada Foundation for Innovation (CFI) and the British Columbia Knowledge Development Fund (BCKDF), and the University of Victoria for instrumentation and operational funding. DMC thanks the University of Victoria for a graduate fellowship. We thank Dr Lisa Rosenberg and Dr Brian Fowler for useful discussions, and the referees for their very helpful suggestions.

## References

- 1 A. T. Lubben, J. S. McIndoe and A. S. Weller, *Organometallics*, 2008, **27**, 3303.
- 2 M. A. Henderson and J. S. McIndoe, *Chem. Commun.*, 2006, 2872.
- 3 P. J. Dyson and J. S. McIndoe, *Inorg. Chim. Acta*, 2003, **354**, 68.
- 4 P. J. Dyson, J. S. McIndoe and D. Zhao, *Chem. Commun.*, 2003, 508.
- 5 J. B. Fenn, M. Mann, C. K. Meng, S. F. Wong and C. M. Whitehouse, *Science*, 1989, **246**, 64.
- 6 R. B. Cole, *Electrospray Ionization Mass Spectrometry: Fundamentals, Instrumentation, and Applications*, John Wiley & Sons, New York, USA, 1997.
- 7 M. N. Eberlin, *Eur. J. Mass Spectrom.*, 2007, **13**, 19.
- 8 N. Taccardi, R. Paolillo, V. Gallo, P. Mastrorilli, C. F. Nobile, M. Raisanen and T. Repo, *Eur. J. Inorg. Chem.*, 2007, 4645.
- 9 A. B. Chaplin and P. J. Dyson, *Organometallics*, 2007, **26**, 2447.
- 10 P. A. Enquist, P. Nilsson, P. Sjöberg and M. Larhed, *J. Org. Chem.*, 2006, **71**, 8779.
- 11 C. Vicent, M. Viciano, E. Mas-Marza, M. Sanau and E. Peris, *Organometallics*, 2006, **25**, 3713.
- 12 L. S. Santos and J. O. Metzger, *Angew. Chem., Int. Ed.*, 2006, **45**, 977.
- 13 D. Feichtinger, D. A. Plattner and P. Chen, *J. Am. Chem. Soc.*, 1998, **120**, 7125.
- 14 P. Chen, *Angew. Chem., Int. Ed.*, 2003, **42**, 2832.
- 15 R. A. J. O'Hair, *Chem. Commun.*, 2006, 1469.
- 16 D. K. Bohme and H. Schwarz, *Angew. Chem., Int. Ed.*, 2005, **44**, 2336.
- 17 W. Henderson and J. S. McIndoe, *Mass Spectrometry of Inorganic and Organometallic Compounds: Tools, Techniques, Tips*, Wiley, Chichester, UK, 2005.
- 18 P. Espinet and K. Soulantica, *Coord. Chem. Rev.*, 1999, **193–195**, 499.
- 19 P. Braunstein and F. Naud, *Angew. Chem., Int. Ed.*, 2001, **40**, 680.
- 20 J. A. Gladysz, D. P. Curran, and I. T. Horvath, *Handbook of Fluorous Chemistry*, Wiley-VCH, Weinheim, Germany, 2004.
- 21 D. M. Chisholm and J. S. McIndoe, *Dalton Trans.*, 2008, 3933.
- 22 C. Decker, W. Henderson and B. K. Nicholson, *J. Chem. Soc., Dalton Trans.*, 1999, 3507.
- 23 N. J. Farrer, R. McDonald and J. S. McIndoe, *Dalton Trans.*, 2006, 4570.
- 24 N. J. Farrer, T. Piga and J. S. McIndoe, *Polyhedron*, 2009, DOI: 10.1016/j.poly.2009.08.013.
- 25 C. Ercolani, J. V. Quagliano and L. M. Vallarino, *Inorg. Chim. Acta*, 1969, **3**, 421.
- 26 V. L. Goedken, J. V. Quagliano and L. M. Vallarino, *Inorg. Chem.*, 1969, **8**, 2331.
- 27 C. Ercolani, J. V. Quagliano and L. M. Vallarino, *J. Chem. Soc. D*, 1969, 1094.
- 28 D. Berglund and D. W. Meek, *J. Am. Chem. Soc.*, 1968, **90**, 518.
- 29 D. Berglund and D. W. Meek, *Inorg. Chem.*, 1969, **8**, 2602.
- 30 R. C. Taylor, R. L. Keiter and L. W. Cary, *Inorg. Chem.*, 1974, **13**, 1928.
- 31 J. F. Young, J. A. Osborn, F. H. Jardine and G. Wilkinson, *Chem. Commun.*, 1965, 131.
- 32 J. A. Osborn, F. H. Jardine, J. F. Young and G. Wilkinson, *J. Chem. Soc. A*, 1966, 1711.
- 33 J. Halpern, T. Okamoto and A. Zakhariyev, *J. Mol. Catal.*, 1977, **2**, 65.
- 34 P. Meakin, C. A. Tolman and J. P. Jesson, *J. Am. Chem. Soc.*, 1972, **94**, 3240.

- 35 J. M. Brown, P. L. Evans and A. R. Lucy, *J. Chem. Soc., Perkin Trans. 2*, 1987, 1589.
- 36 J. P. Collman, L. S. Hegedus, J. R. Norton and R. G. Finke, *Principles and Applications of Organotransition Metal Chemistry*, University Science Books, 1987.
- 37 G. O. Spessard and G. L. Miessler, *Organometallic Chemistry*, Prentice Hall, New Jersey, USA, 1997.
- 38 R. H. Crabtree, *The Organometallic Chemistry of the Transition Metals*, John Wiley & Sons, 2001.
- 39 B. R. James, *Homogeneous Hydrogenation*, John Wiley & Sons, New York, USA, 1973.
- 40 S. B. Duckett, C. L. Newell and R. Eisenberg, *J. Am. Chem. Soc.*, 1993, **115**, 1156.
- 41 S. B. Duckett, C. L. Newell and R. Eisenberg, *J. Am. Chem. Soc.*, 1994, **116**, 10548.
- 42 A. V. Rivera, D. Gomez, E. R. Degil and T. Suarez, *Acta Crystallogr., Sect. C: Cryst. Struct. Commun.*, 1988, **44**, 277.
- 43 R. Fetouaki, A. Seifert, M. Bogza, T. Oeser and J. Blumel, *Inorg. Chim. Acta*, 2006, **359**, 4865.
- 44 L. J. Farrugia, *J. Appl. Crystallogr.*, 1997, **30**, 565.
- 45 H. Arai and J. Halpern, *J. Chem. Soc. D*, 1971, 1571.
- 46 D. R. Eaton and S. R. Stuart, *J. Am. Chem. Soc.*, 1968, **90**, 4170.
- 47 W. Henderson and C. Evans, *Inorg. Chim. Acta*, 1999, **294**, 183.
- 48 N. B. Cech and C. G. Enke, *Mass Spectrom. Rev.*, 2001, **20**, 362.
- 49 C. P. G. Butcher, A. Dinca, P. J. Dyson, B. F. G. Johnson, P. R. R. Langridge-Smith and J. S. McIndoe, *Angew. Chem., Int. Ed.*, 2003, **42**, 5752.
- 50 C. P. G. Butcher, P. J. Dyson, B. F. G. Johnson, P. R. R. Langridge-Smith, J. S. McIndoe and C. Whyte, *Rapid Commun. Mass Spectrom.*, 2002, **16**, 1595.
- 51 J. Halpern and C. S. Wong, *J. Chem. Soc., Chem. Commun.*, 1973, 629.
- 52 F. H. Jardine, J. A. Osborn and G. Wilkinson, *J. Chem. Soc. A*, 1967, 1574.
- 53 M. A. Henderson, S. Kwok and J. S. McIndoe, *J. Am. Soc. Mass Spectrom.*, 2009, **20**, 658.
- 54 T. Waters, R. A. J. O'Hair and A. G. Wedd, *J. Am. Chem. Soc.*, 2003, **125**, 3384.
- 55 D. Schroder, H. Schwarz, D. E. Clemmer, Y. M. Chen, P. B. Armentrout, V. I. Baranov and D. K. Bohme, *Int. J. Mass Spectrom. Ion Processes*, 1997, **161**, 175.
- 56 C. Adlhart, C. Hinderling, H. Baumann and P. Chen, *J. Am. Chem. Soc.*, 2000, **122**, 8204.
- 57 M. A. O. Volland, C. Adlhart, C. A. Kiener, P. Chen and P. Hofmann, *Chem.–Eur. J.*, 2001, **7**, 4621.
- 58 Y. M. Kim and P. Chen, *Int. J. Mass Spectrom.*, 1999, **185–187**, 871.